ISSN 1063-7710, Acoustical Physics, 2016, Vol. 62, No. 6, pp. 717–728. © Pleiades Publishing, Ltd., 2016.
Original Russian Text © G.N. Kuznetsov, O.V. Lebedev, A.N. Stepanov, 2016, published in Akusticheskii Zhurnal, 2016, Vol. 62, No. 6, pp. 699–711.

OCEAN ACOUSTICS. HYDROACOUSTICS

Vertical Amplitude Phase Structure of a Low-Frequency Acoustic Field in Shallow Water

G. N. Kuznetsov[a], O. V. Lebedev[a†], and A. N. Stepanov[b]

[a] *Wave Research Center, Prokhorov General Physics Institute, Russian Academy of Sciences, ul. Vavilova 38, Moscow, 119991 Russia*

[b] *Samara State Aerospace University, Moskovskoe shosse 34, Samara, 443086 Russia*

e-mail: skbmortex@mail.ru

Received July 24, 2015

Abstract—We obtain in integral and analytic form the relations for calculating the amplitude and phase characteristics of an interference structure of orthogonal projections of the oscillation velocity vector in shallow water. For different frequencies and receiver depths, we numerically study the source depth dependences of the effective phase velocities of an equivalent plane wave, the orthogonal projections of the sound pressure phase gradient, and the projections of the oscillation velocity vector. We establish that at low frequencies in zones of interference maxima, independently of source depth, weakly varying effective phase velocity values are observed, which exceed the sound velocity in water by 5–12%. We show that the angles of arrival of the equivalent plane wave and the oscillation velocity vector in the general case differ; however, they virtually coincide in the zone of the interference maximum of the sound pressure under the condition that the horizontal projections of the oscillation velocity appreciably exceed the value of the vertical projection. We give recommendations on using the sound field characteristics in zones with maximum values for solving range-finding and signal-detection problems.

Keywords: shallow water, low frequencies, interference maxima of a vector-scalar field, phase gradient, effective phase velocity, equivalent plane wave, orthogonal projections of the oscillation velocity, variability of a field depending on frequency, distance, and depth levels of emission and reception

DOI: 10.1134/S1063771016050092

INTRODUCTION

In the free space, waves of various type propagate without reflections or limits. In particular, plane waves propagate, retaining the phase synchronism of the pressure and oscillation velocity, and the wave propagation direction coincides with the sound pressure phase gradient. In a real waveguide, e.g., in shallow water, a field interference structure forms that depends on different factors and is difficult to predict, bur with a certain degree of approximation, it can be described by a multiray or multimode model. Here, the phase synchronism of the sound pressure and different projections of the oscillation velocity vector are violated.

Despite the complexity of approximating the field structure with simple functions, the authors of [1] expressed a hypothesis on the possibility of applying a "plane wave" model to approximately describe the field characteristics. Similar ideas are discussed in [2]. In [3], this hypothesis was developed for zones of interference maxima $P_{\max}$. It has been established that the sound pressure phase gradients φ in these zones can be approximately described by the approximating dependence of the "effective phase velocity" $C_\varphi^* = \sum_{l=1} C_{\varphi l} W_l^2 \Big/ \sum_{l=1} W_l^2$, where $C_{\varphi l}$ is the phase velocity of the lth normal wave and W_l is its amplitude. In a similar way, it is also possible to write the relation for the effective (weight average) group velocity $C_g^* = \sum_{l=1} C_{gl} W_l^2 \Big/ \sum_{l=1} W_l^2$, where C_{gl} is the group velocity of the lth normal wave. It is assumed that, using the expressions for C_φ^* in $P_{\max}$ zones at spatially separated points, it is possible to approximately calculate the phase differences for tonal signals, and using C_g^*, to estimate the group delay times for pulse signals. Clearly, C_φ^* and C_g^* are $C_{\varphi,g}^*(r, \omega, h, z, z_0)$, and $C_\varphi^* C_g^* \approx C_0^2$, where C_0 is the sound velocity in water. From here on, r is the distance between the emitter and receiver, $\omega = 2\pi f$ is the circular frequency, h is the depth of the waveguide, z and z_0 are the depths of the receivers and emitter, and f is the frequency of the sound signal.

In [4], these problems are analyzed numerically for different hydrophysical conditions of sound propaga-

† Deceased.

tion in a waveguide. It is shown that with an increase in distance, C_φ^* tends toward a constant value, but a natural dependence on the hardness of the bottom and the sound frequency is observed. In [5], it has been established that, using quantity C_φ^* (further, C^*) instead of the sound velocity in water C_0 and signal processing at frequencies for which the array is located in the $P_{\max}$ zone, the directional characteristic (DC) of the array gives unbiased bearing estimates γ and the lateral field has no "spikes." And vice versa, when the array aperture is located in the zone of interference minima of the field $P_{\min}$, the DC splits, the bearing estimates are displaced, and the lateral field increases. Displacement of bearing estimate γ when using C_0 instead of C^* seems natural, since quantity C_0 does not agree with the real sound pressure (SP) phase gradients at the array aperture.

On the whole, the results presented in [4, 5] make it possible to give practical recommendations on using the effective velocity C^* as an analog of the phase velocity of the "equivalent plane wave" (EPW) characterizing the local phase gradients in the $P_{\max}$ zone. Instead of the sound velocity in water C_0, it is recommended to use C^* values when forming the DC of an array located in the zone of the maximum.

This velocity can be estimated approximately using the above formula, which takes into account all modes propagating in the waveguide, or only the groups of the most coherent modes with close wavenumbers. The dependences $C^*(r, \omega, h, z, z_0)$ can also be determined numerically using an adequate model, e.g., the multimode acoustic waveguide model, or they can be measured experimentally by estimating the spatial phase gradient in the horizontal plane, $C^* = \omega/(\partial\varphi/\partial r)$.

However, it should be noted than in [1–5], only the characteristics of scalar fields are discussed, whereas today, research into vector-phase (vector-scalar) fields are also important [6, 7]. In addition, in [4, 5], the characteristics of the SP field are considered only in the horizontal plane; the dependences on depth z and z_0 have not been studied.

Below, for a low-mode waveguide, we analyze the spatial frequency amplitude-phase SP characteristics $P(r, \omega, h, z, z_0)$ (further P), the horizontal and vertical projections of the SP phase gradient vector, and the oscillation velocity vector (OVV).

1. DEFINING MATHEMATICAL RELATIONS

1.1. Theoretical Models of the Vector-Scalar Field in a Waveguide

Let us consider a point directional harmonic source, the sound potential of which in a nonorganic space has the form $\psi = \psi_0 e^{-i\omega t}$, where ψ_0 is the cofactor of the potential, which is independent of time t, and i is an imaginary unit. Under the hypothesis of the potential character of the field, the relationship between the oscillation velocity $\mathbf{V}$ and SP P is expressed by unknown relations [8]: $\mathbf{V} = \operatorname{grad}\psi$, $P = -\rho_0 \dfrac{\partial\psi}{\partial t} = i\omega\rho_0\psi$, where ρ_0 is the density of the medium.

Let $P = |P| e^{i\varphi} = \operatorname{Re} P + i \operatorname{Im} P$, where $|P|$ is the modulus, $\varphi = \arg P$ is the argument, $\operatorname{Re} P$ is the real part, and $\operatorname{Im} P$ is the imaginary part of SP P.

$$\frac{\partial\varphi}{\partial x} = \frac{\operatorname{Re} V_x \operatorname{Re} P + \operatorname{Im} V_x \operatorname{Im} P}{|P|^2/\omega\rho_0},$$

$$\frac{\partial\varphi}{\partial y} = \frac{\operatorname{Re} V_y \operatorname{Re} P + \operatorname{Im} V_y \operatorname{Im} P}{|P|^2/\omega\rho_0},$$

$$\frac{\partial\varphi}{\partial z} = \frac{\operatorname{Re} V_z \operatorname{Re} P + \operatorname{Im} V_z \operatorname{Im} P}{|P|^2/\omega\rho_0},$$

where $\operatorname{Re} V_x$, $\operatorname{Im} V_x$, $\operatorname{Re} V_y$, $\operatorname{Im} V_y$, $\operatorname{Re} V_z$, $\operatorname{Im} V_z$ are the real and imaginary parts of the corresponding components of vector $\mathbf{V}$. Similar relations for different projections of the phase gradient $\operatorname{grad}\varphi$ of the SP can also be obtained using the relation $\operatorname{grad}\varphi = (\operatorname{Re} P \operatorname{grad} \operatorname{Im} P - \operatorname{Im} P \operatorname{grad} \operatorname{Re} P)/|P|^2$ [9].

To find the fields of pressure P in a Pekeris waveguide, we use the well-known integral representation for the potential of the field of a point nondirectional emitter in the form [8, 10]:

$$\psi_0 = A \int_{-\pi/2+i\infty}^{\pi/2-i\infty} H_0^{(1)}(kr\sin\vartheta) F(\vartheta) \sin\vartheta \, d\vartheta, \qquad (1)$$

where A is the volumetric velocity of the source, $H_0^{(1)}(kr\sin\vartheta)$ is the zero-order Hankel function of the first kind, k is the wavenumber, and $r = \sqrt{(x-x_0)^2 + (y-y_0)^2}$ is the horizontal distance between the emitter and the reception point,

$$F(\vartheta) = \begin{cases} -\dfrac{\left(e^{-bh+bz_0} + V_1(\vartheta) e^{bh-bz_0}\right)\left(e^{bz} - e^{-bz}\right)}{e^{-bh} + V_1(\vartheta) e^{bh}}, \\ 0 \le z \le z_0, \\ -\dfrac{\left(e^{bz_0} - e^{-bz_0}\right)\left(e^{-bh+bz} + V_1(\vartheta) e^{bh-bz}\right)}{e^{-bh} + V_1(\vartheta) e^{bh}}, \\ z_0 \le z \le h, \end{cases}$$

$b = ik\cos\vartheta$, $V_1(\vartheta)$ is the coefficient of reflection from the bottom of the waveguide.

Since integral (1) converges uniformly outside a certain arbitrarily small vicinity within which the source is located, the components of OVV $\mathbf{V}$ can be found by direct differentiation of (1) over the corre-

sponding coordinates. As a result, we obtain the following expression for the orthogonal OVV projections of the considered source in a Pekeris waveguide:

$$V_x = \frac{-Akx}{r}\int_G H_1^{(1)}(u)F(\vartheta)\sin^2\vartheta d\vartheta,$$
$$V_y = \frac{-Aky}{r}\int_G H_1^{(1)}(u)F(\vartheta)\sin^2\vartheta d\vartheta, \qquad (2)$$
$$V_z = \frac{ikA}{2}\int_G H_0^{(1)}(u)F_z(\vartheta)\sin 2\vartheta d\vartheta,$$

where $G = (-\pi/2 + i\infty, \pi/2 - i\infty)$, $u = kr\sin\vartheta$,

$$F_z(\vartheta) = \begin{cases} -b\dfrac{\left(e^{-bh+bz_0} + V_1(\vartheta)e^{bh-bz_0}\right)\left(e^{bz} + e^{-bz}\right)}{e^{-bh} + V_1(\vartheta)e^{bh}}, \\ 0 \le z \le z_0, \\ -\dfrac{\left(e^{bz_0} - e^{-bz_0}\right)\left(e^{-bh+bz} - V_1(\vartheta)e^{bh-bz}\right)}{e^{-bh} + V_1(\vartheta)e^{bh}}, \\ z_0 \le z \le h. \end{cases}$$

Integrals (1), (2) can be calculated by direct numerical integration or the saddle point method. In addition, using the standard calculation technique (2), integrals (2) can be reduced to sums analogous to those of normal waves of the SP field:

$$P = i\omega\rho_0\sum_{l=0}^{\infty} A_l H_0^{(1)}(r\xi_l), \quad V_x = \frac{-x}{r}\sum_{l=0}^{\infty} A_l\xi_l H_1^{(1)}(r\xi_l),$$
$$V_y = \frac{-y}{r}\sum_{l=0}^{\infty} A_l\xi_l H_1^{(1)}(r\xi_l), \quad V_z = \sum_{l=0}^{\infty} A_l' H_0^{(1)}(r\xi_l), \qquad (3)$$

where $u_l = h\sqrt{k^2 - \xi_l^2}$; ζ_l, $l = 0,1,2,\ldots$ are the roots of the dispersion equation of the Pekeris waveguide $\operatorname{cotan} x = i\sqrt{x^2 - (kh\nu)^2}/mx, m = \rho/\rho_0$ is the ratio of the densities of water and the underlying half-space, $\nu^2 = 1 - n^2$, $n = n_0(1 + i\tilde{\alpha})$, $n_0 = c_0/c$ is the ratio of the sound velocities in the waveguide and bottom, $\tilde{\alpha}$ is the boundary absorption coefficient, $\alpha_{l0} = u_l z_0/h$, $\alpha_l = u_l z/h$,

$$A_l = -\frac{2A\pi u_l \sin\alpha_{l0}\sin\alpha_l}{h(\sin^2 u_l \tan u_l/\tilde{m}^2 + \sin u_l \cos u_l - u_l)},$$
$$A_l' = A_l u_l \operatorname{cotan}\alpha_l/h.$$

The calculations presented below for substantiating the calculation accuracy were carried out using contour integration and an analog for decomposition of the SP by normal waves, applied to the OVV components (see (2) and (2)). The results of calculations for $r > h$ virtually correspond; therefore, further, we present the dependences calculated only by decomposition by normal waves.

1.2. Initial Data and Notation Used in Calculations

Let us consider the field characteristics of a point directional source in a Pekeris waveguide, which is a homogeneous water layer with a thickness of $h = 100$ m with a sound velocity in water of $C_0 = 1450$ m/s. We perform calculations for the following bottom parameters: $m = 1.8$; $n = 0.725$; attenuation coefficient $\tilde{\alpha} = 0.02$.

We superpose the plane *OKY* of the coordinate system with the free surface of the waveguide; the *OZ* axis is directed downward toward the bottom of the waveguide. We place the emitter and depth z_0, and the horizontal coordinates of the emitter are equal to zero: $x_0 = 0$ and $y_0 = 0$. We place a four-component vector-scalar sound receiver (or multielement array) in the horizontal plane at a distance from the emitter of $x = 5$ and 20 km. We take receiver depths equal to $z = 50$ and 100 m. We consider that $y = 0$ and $r = x$, since $r \gg h$.

Let us study the amplitude-phase characteristics of the vertical-scalar field in the waveguide in the interests of solving problems on detection and range-finding of weak signals against an interference background. For this, we analyze the interference structure of the field, primarily in the $P_{\max}$ zones. Below, in contrast to [4, 5], the main focus is on the dependences of the field characteristics on the quantities z and z_0. We also study in the $P_{\max}$ and $P_{\min}$ zones the source depth dependences of the effective phase velocity value, which characterize the local phase gradients in the horizontal plane.

In Figs. 1–6, the following curve designations are introduced: *1*, SP amplitude $|P|$; *2*, effective phase velocity, calculated from the horizontal projection of the phase gradient of the SP field, $C_1^* = \omega/(\partial\varphi/\partial r)$; *3*, effective phase velocity, calculated from the approximate formula $C_2^* = \sum_{l=1} C_{\varphi l} W_l^2 / \sum_{l=1} W_l^2$; *4*, horizontal projection of the phase gradient $\varphi_r' = \dfrac{\partial\varphi}{\partial r}$; *5*, vertical component of the phase gradient $\varphi_z' = \dfrac{\partial\varphi}{\partial z}$; *6*, horizontal projection of the OVV V_r; *7*, vertical projection of oscillation velocity V_z; *8*, angle between direction of SP phase gradient vector and horizontal plane $\xi = \arctan\varphi_z'/\varphi_r'$, which in the $P_{\max}$ zones can be considered as the angle of arrival (grazing angle) of the EPW, which approximates the SP field in this zone; *9*, the angle between the direction of the OVV and the horizontal plane $\zeta = \arctan V_z/V_r$; *10* is the SP phase $\varphi = \arg P$; *11*, the phase of the horizontal component of the OVV $\arg V_r$; *12*, the phase of the vertical

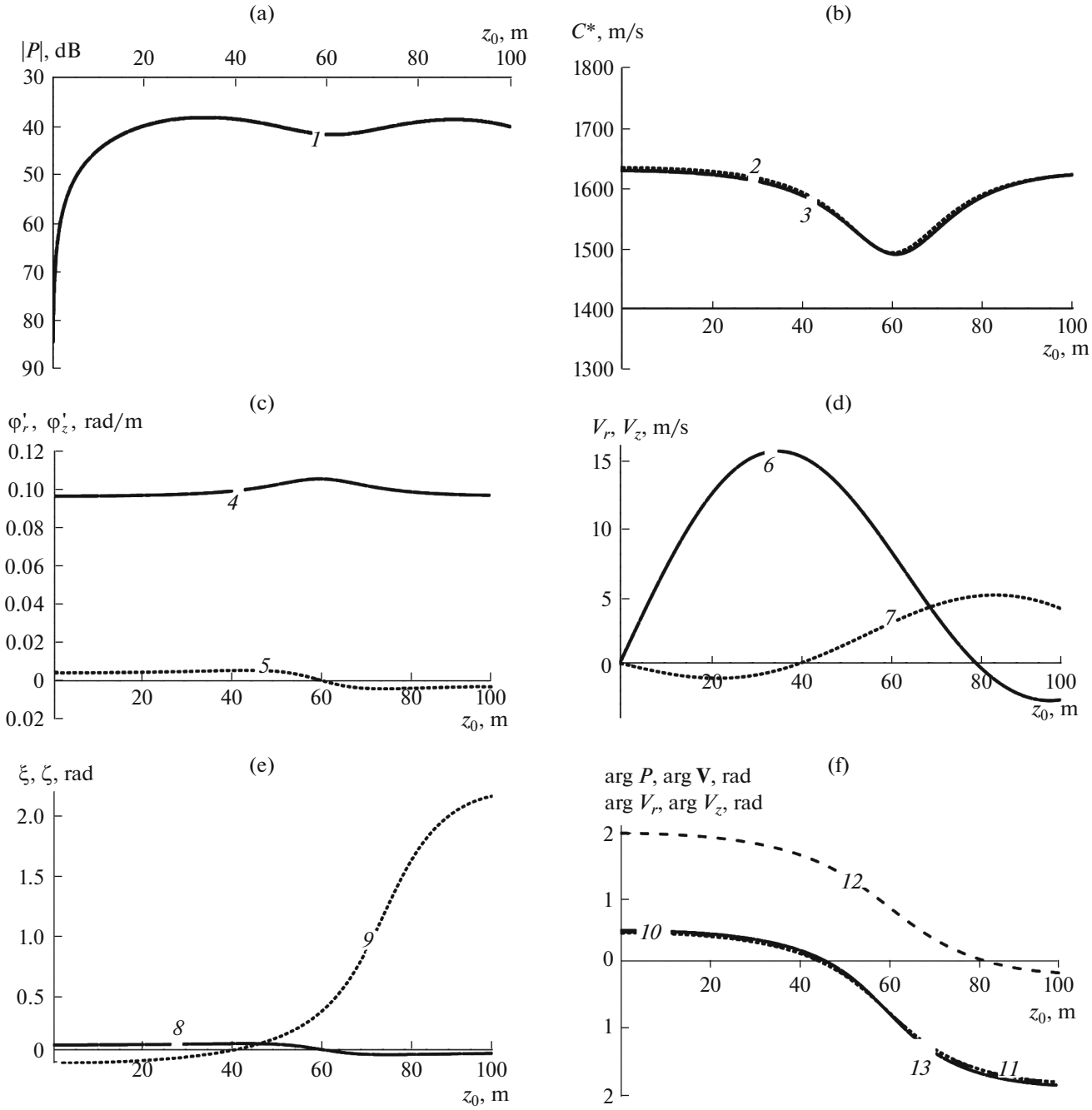

Fig. 1. Sound field characteristics depending on z_0 for $f = 25$ Hz, $r = 5$ km, $z = 100$ m.

component of the oscillation velocity $\arg V_z$; *13*, the phase of the total OVV $\arg \mathbf{V}$. Note that the angle ξ is related to the EPW angle of incidence θ to the horizontal by the obvious relation $\theta = \pi/2 - \arctan\varphi'_z/\varphi'_r$. We also take into account the fact that the projections of the OVV correspond not to the amplitudes, but to the real part; i.e., phases are taken into account.

Figures 1–6 present the following plots: (a) pressure amplitude $|P|$; (b) effective phase velocities C_1^* and C_2^*; (c) horizontal and vertical projections of the phase gradient vector φ'_r and φ'_z, (d) the same projections of the OVV V_r and V_z; (e) direction of phase gradient of SP ξ and OVV ζ; (f) the phases of the SP $\arg P$, of the horizontal projection of the oscillation velocity $\arg V_x$, of the vertical projection of the oscillation velocity

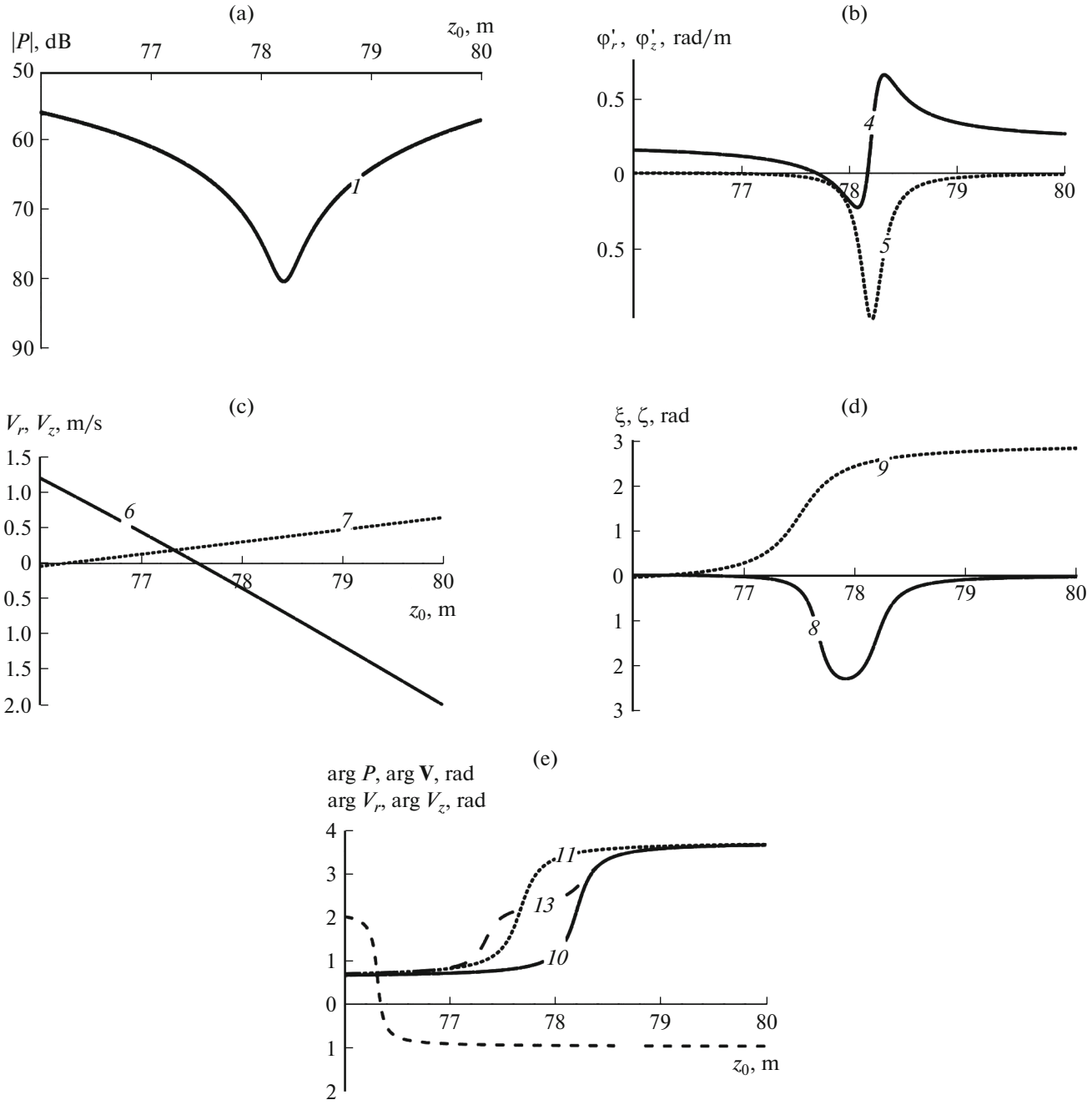

Fig. 2. Sound field characteristics depending on z_0 for $f = 50$ Hz, $r = 5$ km, $z = 100$ m.

$\arg V_z$ and of the OVV $\arg \mathbf{V}$, which are counted from the given reference value near the emission point.

From the above designations it follows we have posed the problem of studying the source depth dependences of the effective phase velocities and the angular characteristics of the phase gradient of the SP and OVV (characteristics ξ and ζ). It is assumed that vector ξ is orthogonal to the EPW front. It is necessary to calculate the listed characteristics to analyze the algorithms that use "power flow" signal processing [6, 7].

2. STUDY OF THE INTERFERENCE AND PHASE STRUCTURE OF A LOW-FREQUENCY FIELD IN A PEKERIS WAVEGUIDE

2.1. Simulating the Characteristics of a Sound Field in the Near-Bottom Region

Studying this problem is interesting for analysis of the signal characteristics at the aperture of spatially developed bottom hydrophysical scalar or vector-scalar arrays.

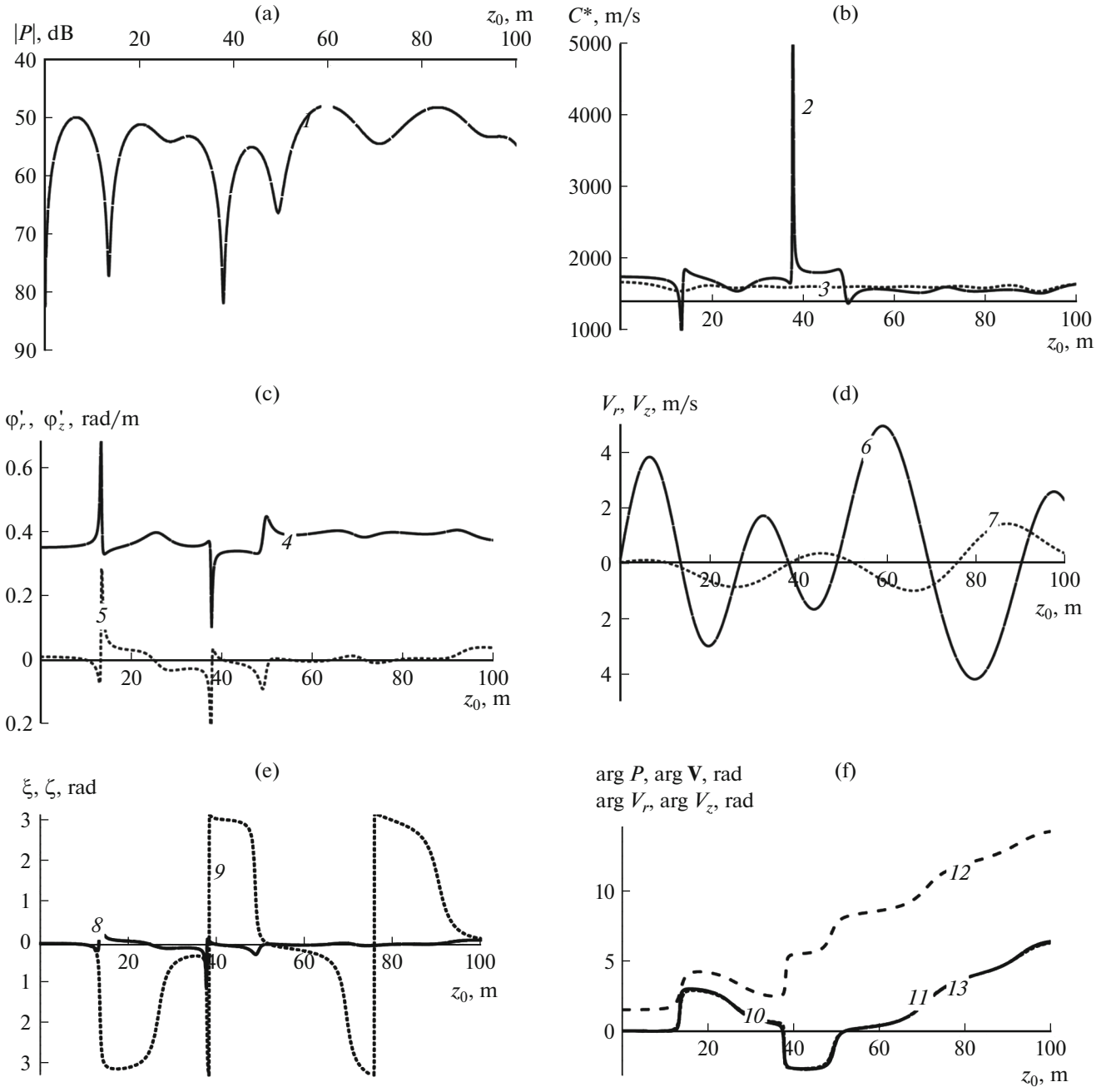

Fig. 3. Sound field characteristics depending on z_0 for $f = 100$ Hz, $r = 5$ km, $z = 100$ m.

Receiver depth 100 m, distance to source 5 km. Figure 1 shows the calculation data for a frequency of $f = 25$ Hz, at which signals propagate with two normal waves. Clearly, near the free surface, the quantities P, V_r, and V_z rapidly decrease. A shallow interference SP minimum ($P_{\min}$) formed at a depth of 62 m, corresponding to the middle of the effective width of the waveguide $h^* = h + \Delta h = 124.13$ m [13]. In the given conditions of near-bottom signal reception, the C^* values calculated by the longitudinal component of the phase gradient $C_1^* = \omega(\partial\varphi/\partial r)^{-1}$ and by the approximate formula (Fig. 1b, curves *2* and *3*) practically coincide, independently of the source depth.

It is clear that in the $P_{\max}$ zones, the $C_{1,2}^*$ values are appreciably larger than the sound velocity in water C_0, and only in the $P_{\min}$ zone do they tend to C_0. Therefore, bottom-moored or towed horizontal arrays, in order to obtain an unbiased bearing during DC formation, should take into account the source depth depen-

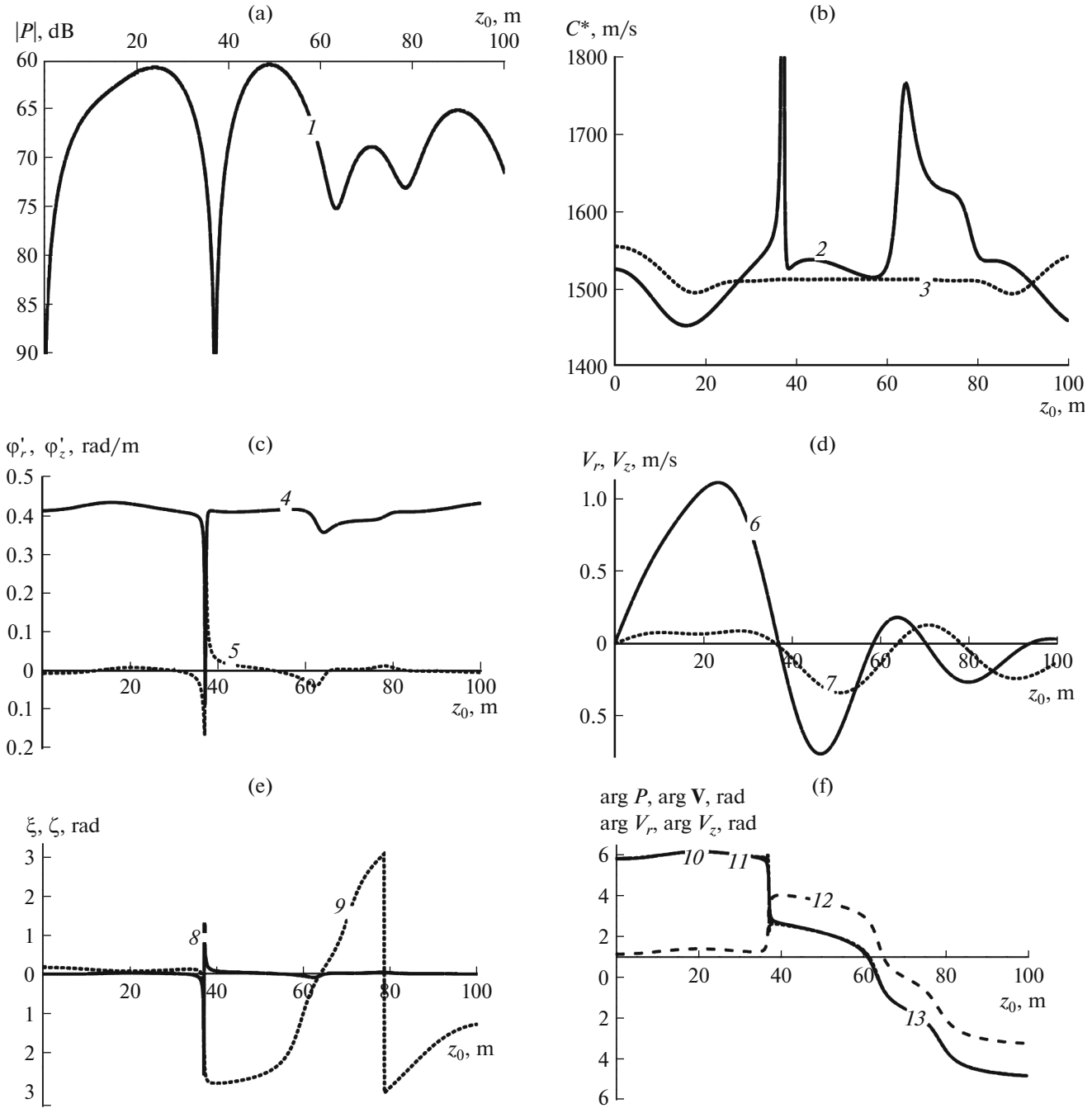

Fig. 4. Sound field characteristics depending on z_0 for $f = 100$ Hz, $r = 20$ km, $z = 100$ m.

dences of the phase gradient at the aperture. For this, it is necessary to use the quantities C_1^* or C_2^*.

For vertical emitting arrays, the phase gradients in the vertical plane are necessary. These characteristics are shown in Fig. 1c, and the OVV projections are shown in Fig. 1d. One can see that in the $P_{\min}$ zone, the horizontal component of the phase gradient φ'_r forms a maximum, and the vertical component of the gradient φ'_z changes sign. Accordingly, there is a change in the direction and value of the EPW angle of arrival.

From analysis of the curves in Fig. 1, it follows that for the given conditions—distance, waveguide depth (100 m), bottom characteristics, and frequency of 25 Hz—when the source is located at depths less than 62 m (the middle of the equivalent waveguide), normal waves at the reception point are summed such that the

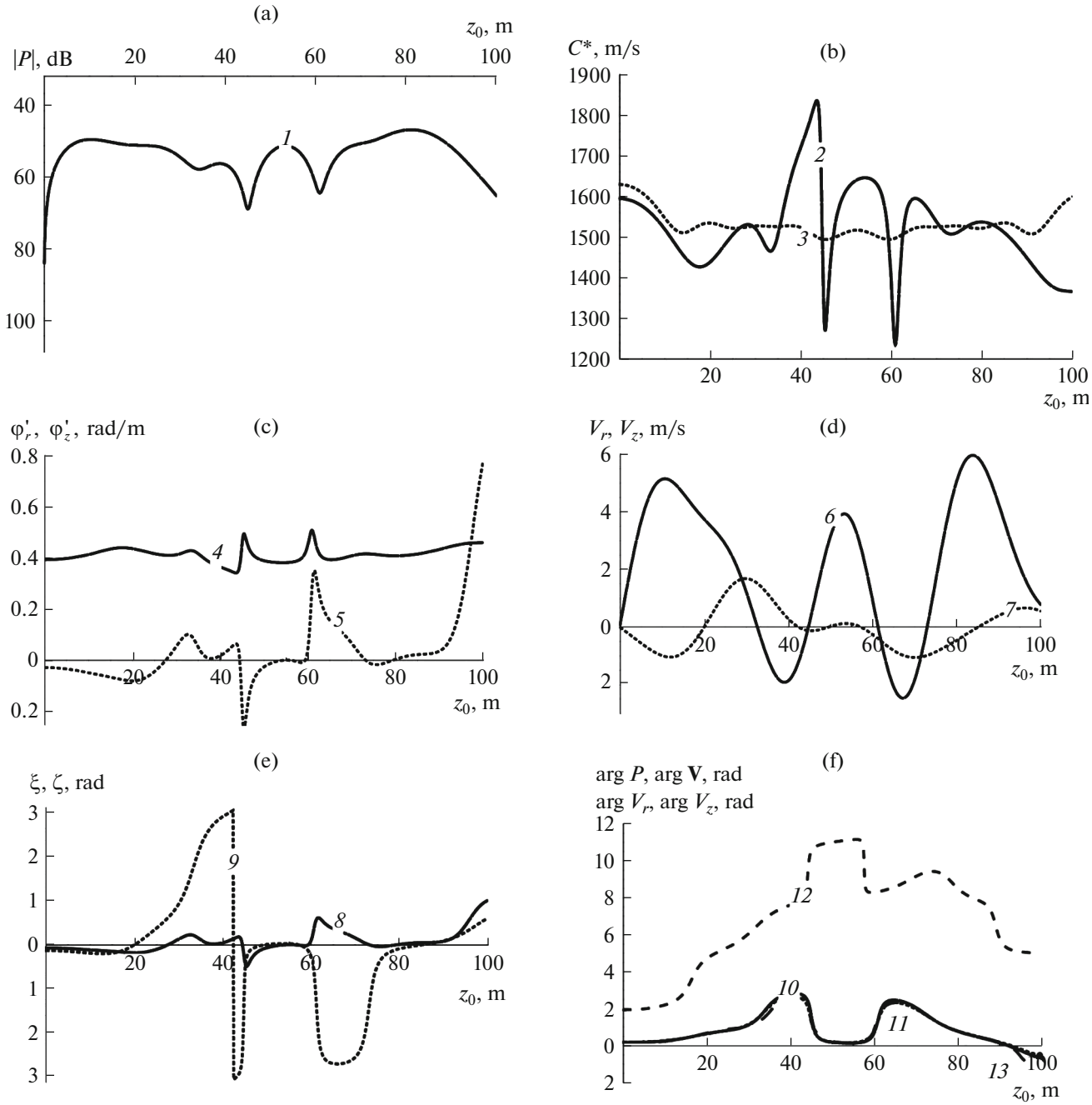

Fig. 5. Sound field characteristics depending on z_0 for $f = 100$ Hz, $r = 5$ km, $z = 50$ m.

EPW arrives "from above" ($\xi > 0$). When the source is located at depths greater than 62 m, the EPW arrives "from below" ($\xi < 0$). The range of variation in the EPW angles of arrival in this case is not large, from $-2.3°$ to $+3.2°$. Accordingly, for $\xi = 0$, the SP wave front is perpendicular to the horizontal direction.

A difference in the values and directions of the EPW angles of arrival ξ and values and directions of the angle of arrival of the OVV ζ is observed.

Note that arg V_z differs from arg P, arg V_r, and arg $\mathbf{V}$ by almost 90°; i.e., projection V_r is "active"—coinciding in phase with P; and projection V_z is "reactive." It is essential that the amplitude V_z is appreciably smaller than the amplitude V_r; therefore, from here on, the phases of P and the total vector $\mathbf{V}$ are also close and their dependences on z_0 virtually coincide.

With a change in distance r, frequency f, or receiver depth z, with all other conditions being equal, the

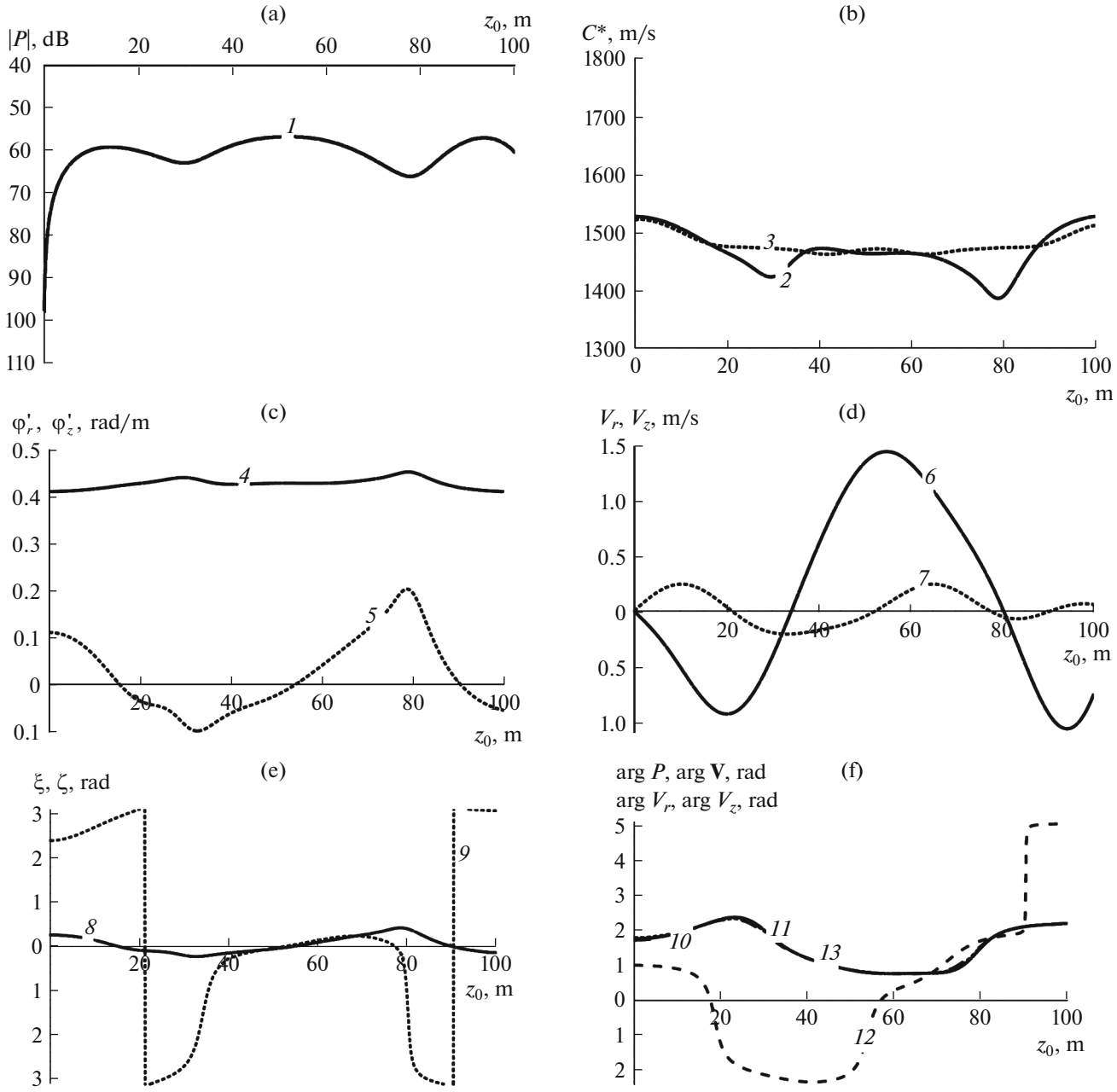

Fig. 6. Sound field characteristics depending on z_0 for $f = 100$ Hz, $r = 20$ km, $z = 50$ m.

structure of the SP field can substantially change; in particular, zones with deep interference minima can occur. This is confirmed by the results presented in Fig. 2, which were obtained for a frequency of $f = 50$ Hz, at which in the considered waveguide five normal waves propagate. As a result, the interference structure of the field due to the increase in the number of modes became more complex and, in particular, it was discovered that at the given distance for an emitter located at a depth of $z_0 = 78.2$ m at a near-bottom reception point, a "singularity" formed: a sharp, deep minimum in the SP amplitude is observed. In the vicinity of the maximum, in contrast to Fig. 1, one can see sharp jumps in the phases and phase gradients in the vertical and horizontal planes. For a detailed analysis of the field characteristics in this zone (depth range of 76–80 m), more detailed calculations have been carried out.

One can see that in the narrow zone $P_{\min}$ (Fig. 2a), for a change in emitter depth z_0, the projections of the SP phase gradient (Fig. 2c, curves *4* and *5*) and the angle of arrival of the SP front ξ (Fig. 2e, curve *8*) experience a jump by, respectively, $\pi/2$ and π radian.

Note that the depth level of the SP minimum (78.2 m) does not coincide with the depth levels of the minima of the phase gradient projections (76.3 and 77.7 m), but the jump in the SP phase is at the same depth (78.2 m, Fig. 2f, curve *10*).

Note that in the general case, the directions of the OVV and EPW differ, but for $|V_r| > |V_z|$, the difference in angles does not exceed 5°–10°; however, in individual zones, they virtually coincide. As calculations show, close results are also observed under other sound field generation conditions: at different frequencies and different distances. The rapid transition from the maximum to minimum value of the SP (and back) with a change in sign in the longitudinal component of the phase gradient φ'_r (Fig. 2c, curve *4*) can correspond to the vertical section near anomalous zones of the vector field of the power flow—vorticity zones, in which, according to [9, 14, 15], singularities of the phase front form: poles (dislocations) and saddles. Vorticity formed as a result of revolution of the local value of the power flow density around a singular point.

The vertical component of the phase gradient φ'_z in this region has an sharp, deep minimum (Fig. 2c, curve *5*), which leads to a deep minimum of the angle of arrival ξ. In this case, the EPW angle of arrival with variation in the source depth by only 1 m changes within the limits of −130° to 0° (Fig. 2e). In the remaining region, it changes insignificantly, from −6° to +2°. For this, the angle of arrival of the OVV ζ changes near the $P_{\min}$ zone by π radian.

As mentioned above, similar anomalies were studied in [9, 14, 15], but for a section of the field in the horizontal plane and an analysis of the dislocation characteristics for a change in distance between the source and receiver. These works show that in the zone of the SP minimum, a change in the direction of the phase gradient and, accordingly, a change in the direction of the power flow vector are possible. In Fig. 2 and further, it is shown that analogous effects are also observed for a change in the vertical coordinates, e.g., for vertical movement of the source or receiver.

Figure 3 shows results analogous to Fig. 1 for a frequency of 100 Hz. From analysis of this figure, it follows that for an increase in the sound frequency, a more jagged interference dependence of the SP field on source depth is formed. The reason for this phenomenon is that with an increase in frequency, the number of normal waves increases, as well as the difference in the wavenumbers.

One can see that in $P_{\max}$ zones, the C_1^* and C_2^* values change weakly and are quite close in value. However, in zones of deep $P_{\min}$ due to an increase or decrease in the phase gradient in the horizontal plane, jumps in C_1^* are observed, both smaller and larger. In zones with a shallow SP minimum, C_1^* tends toward the sound velocity in water. Quantity C_2^* does not take into account local gradients and weakly depends on depth. On average, the effective phase velocities depending on the SP phase gradient in the horizontal plane, independently of the depth level of emission, noticeably exceed quantity C_0. Therefore, if during formation of the DC by vertical arrays, the values of the effective phase velocity are not used, then during detection of sources, a shift in the bearing estimate γ will be observed, especially for glancing angles of wave incidence.

In Figs. 3a and 3c, just like in Fig. 2, one can see that singular points of the phase gradient (singularities) form in the zone of deep SP minima. Curves *4* and *5* in Fig. 3c show the positive and negative "spikes." It can be assumed that in these $P_{\min}$ zones, "neighboring dislocations" formed [9, 14, 15], which have opposite signs of vorticity and form in their zones phase gradients with opposite signs. This is also confirmed by the fact that in the vicinity of the minimum of the vertical projection of the oscillation velocity V_z, the vertical component of the gradient changes φ'_z sign. However, a change in the direction of the phase gradient with movement in the vertical plane is also possible if the point of the pole (dislocation) is "passed around" from the left and right. Such results were obtained in [9, 14, 15] for a change in the coordinates of the reception and emission points in the horizontal plane. In other words, the physical characteristics of the vector-scalar field in the $P_{\max}$ and $P_{\min}$ zones do not depend on the plane in which the coordinates of the receiver or emitter change.

From the presented results, it also follows that for small changes in the parameters characterizing the source coordinates, at singular points, substantial changes in the field characteristics occur at the reception point; i.e., the field at singular points is "especially sensitive" [16]. For example (Fig. 3c), at singular points for a change in source depth by 2–3 m, jumps in the SP phase in the horizontal and vertical planes reach $+\pi$ or $-\pi$. Jumps in φ'_r and φ'_z lead to deviations of the EPW angles of arrival from the horizontal plane within the limits from −62° to +33°. Outside zones of SP minima, the EPW angles of arrival, like before, change insignificantly: from −5° to +3°.

Meanwhile, in the $P_{\min}$ zones, sharp jumps in the direction of the OVV angles of arrival are observed: to values of $\pm\pi$ radian. Essentially, the size and the angle of arrival of the OVV depend not only on the presence or absence of $P_{\max}$ and $P_{\min}$ zones, they are also a function of the relation of amplitudes V_r and V_z. As mentioned above, in the zone corresponding to the relation $|V_r| > |V_z|$, the difference between angles ξ and ζ is not large and does not exceed 10°–12°.

Receiver depth 100 m and distance to source 20 km. This problem is interesting from the viewpoint of evaluating the influence of degeneracy of the mode composition due to the more intense attenuation of higher-number modes. The characteristics of the vector-scalar field were calculated for the same frequencies and in the same waveguide. It has been established that due to attenuation of higher-number modes, the

field structure is mainly determined by the characteristics of the first modes. As a result, the effective velocities C_1^* or C_2^* in P_{max} zones hardly depend at all on depth z_0 or z and always exceed quantity C_0. With an increase in frequency or distance, the difference between C_1^* or C_2^* and C_0 decreases from 15 to 8–10%. From the calculations it also follows that in the case of near-bottom signal reception, the dependences of quantities P, V_r, V_z, and angles ξ and ζ on depth z_0 change slowly with increasing distance.

As an example, Fig. 4 shows the studied dependences on source depth z_0 for a signal at a frequency of 100 Hz. Clearly, in P_{max} zones, the projection of the phase gradient in the horizontal plane and, correspondingly, quantities C_1^* and C_2^* change weakly. However, in the P_{min} zone for an emitter depth of around 37 m, a jump is observed (a decrease to almost a zero value) in the phase gradient in the horizontal plane φ'_r. As a result, quantity C_1^* sharply increases, to an unrealistically large value of 37420 m/s (the effect of division by a small number).

The vertical component of the SP phase gradient at this point has a discontinuity. A jumplike change in the direction of the phase gradient φ'_z and a sign-alternating change in quantities V_r and V_z occur, which in the P_{min} zone leads to a corresponding change in the angles of arrival ξ and ζ. For example, quantity ζ changes within the limits from –96° to 126°. It is possible to assume that the zone of the minimum is located near the singularity of the phase front.

2.2. Simulation of the Field Charateristics with Signal Reception in the Middle of a Waveguide

It is necessary to solve this problem in order to choose the signal processing modes using towed spatially developed hydrophyscial scalar or vector-scalar arrays.

Receiver depth 50 m, distance to source 5 and 20 km. Figures 5 and 6 shows hydrophysical field characteristics analogous to Figs. 1–4, but for a frequency of 100 Hz and distances of 5 and 20 km, respectively.

One can see that, just like in the case of near-bottom reception, as a result of the increase in frequency, the jaggedness of the field increases, but with an increase in distance, the interference of the SP and other characteristics is "smoothed." On the whole, the results of calculations are similar to the previous ones: in P_{max} zones, C_1^* and C_2^* virtually coincide and exceed quantity C_0 by 10–15%. In P_{min} zones, in this case anomalous changes in the phase gradient are formed, and the C_1^* values depending on the real SP phase gradients in the horizontal plane substantially deviate from the mean value, greater or lower. Amplitude V_r noticeably exceeds amplitude V_z. For $|V_r| > |V_z|$ quantities ξ and ζ differ insignificantly.

The range of the change in angles of arrival of OVV ζ for different distances and frequencies can vary within wide limits. For example, in the given case, quantity ζ varies from –29° to +60° for a distance of 5 km and from $-\pi$ to $+\pi$ for distances of 20 km. In P_{min} zones, jumps in the phase gradients and values of ζ are observed. If under the given sound propagation conditions large interference minima of the SP are not observed, then the EPW angles of arrival vary more gradually. Independently of the source depth, in P_{max} zones, an EPW of the SP arrives from directions close to horizontal. For the given receiver depth (50 m) angle of arrival ξ varies from –13° to +24° and deviations are observed only in P_{min} zones. The dependences of the arguments (phases) P, V_r, and $\mathbf{V}$ on source depth z_0, like in the case of near-bottom reception, virtually coincide, but the character of the calculated dependences, as follows from comparison of Figs. 1–4 and Figs. 5 and 6, differ substantially.

CONCLUSIONS

The sound pressures in zones of interference maxima are characterized by weak changes in the phase gradient in the horizontal and vertical planes, which makes it possible to apply the EPW to these zones. Since the phase structures of P and V_r are similar, the EPW is valid in the P_{max} zone for a scalar field and for the horizontal OVV component. This makes it possible to use the EPW model for generation of the DC by horizontal vertical scalar and vector-scalar arrays, as well as for power flow signal processing [6, 7].

The application of the averaged values $C_1^*(\omega, z_0)$ or $C_2^*(\omega, z_0)$ when generating the DC makes it possible with the EPW to partially adapt an array in zones of interference maxima to the sound field model, but with allowance for their dependences on depths z and z_0. In this case, partial agreement of the arrays and averaged characteristics of the waveguide transfer function is achieved.

The quantity of the effective phase velocity characterizing the phase gradients at the array aperture depend on the sound frequency and depths z and z_0. In P_{max} zones, it appreciably exceeds quantity C_0 and is quite stable. As well, the C_1^* and C_2^* values in P_{max} zones are close, which makes it possible to estimate them analytically (C_2^*), numerically, or experimentally (C_1^*). In the zone with shallow minima, quantity C_1^* approaches the value of sound velocity in water C_0.

In the processing of wideband signals and generation of the DC using $C_1^*(\omega, z_0)$ and $C_2^*(\omega, z_0)$, the horizontal array at certain frequencies is always located in the P_{max} zone, which makes it possible at precisely these frequencies, due to coherent combination of sig-

nals at the array aperture, to increase the interference immunity and eliminate shifts in bearings [4, 5].

When the receiver elements are placed in the $P_{\min}$ zones, large gradients and jumps in the phase difference, changes in the direction of the vertical component of the OVV, and changes in the angles of arrival of both the OVV and EPW to the reception point are observed. In the $P_{\min}$ zone, the angles of arrival can vary within the limits of $\pm\pi$, and these changes can have a jumplike character, corresponding to the description of the field behavior near singular points of the phase front [9, 14–16]. However, when solving practical problems, these jumps and variations in direction are insignificant, because at frequencies where the $P_{\min}$ zone forms, signals from a low-noise source cannot be detected due to additive and multiplicative interference. As a result, studies of the field characteristics in the $P_{\min}$ of the SP are predominantly of theoretical interest. The reason for this is also because when an array or part of it is located in the $P_{\min}$ zone, not only a decrease in the signal/noise ratio should be expected at single receivers, but also a decrease in the array's axial concentration coefficient, which is conditioned by unpredictable and large signal phase gradients in this zone. As a result, there should be a reduction in interference immunity and the bearing estimates should deviate from true values.

The features of the field in the $P_{\min}$ zone can be used not only for a large signal/noise ratio, e.g., to check the adequacy of acoustic bottom models or to solve various measurement problems, since localization of the zones of minima and the field characteristics in these zones are "especially sensitive" to variation in the hydrophysical conditions in the waveguide [16]. Note that to solve these problems, four-component vector-scalar receivers can be recommended, which simultaneously record the horizontal and vertical projections of the velocity vector.

Based on these results, it is necessary to carry out theoretical and experimental research of the complex field characteristics SP, V_r, V_z, and $\mathbf{V}$ and the phase gradients in $P_{\max}$ zones. The presence of these zones, which always exist in the field of a wideband signal, makes it possible to efficiently solve problems of detecting and estimating the parameters of a sound source. In such zones, the EPW angles of arrival in large spatial intervals are constant and close to horizontal, which makes it possible to accumulate signal power for a long observation and tracking time.

The gradual dependence of the phase gradients on the location depth of a source in the vertical plane makes it possible in zones of interference maxima to successfully apply vertical arrays, particularly, vector-scalar ones. However, it is necessary to take into account the probable change in the EPW angle of arrival and variation in the signal/noise ratio.

It should also be noted that the real parts P and V_r are in-phase. The phase of the total OVV also virtually coincides with them if $|V_r| > |V_z|$. For this same reason, in the intervals Δz_0, when $|V_r| > |V_z|$, the EPW and OVV angles of arrival differ by no more than 10°–12° (or they coincide). The substantial variability of the vector-scalar field characteristics depending on the depths of the emitter and receiver, as well as the distance and sound frequency, make it possible to draw a conclusion on the need to predict and experimentally study the mentioned characteristics in order to optimize signal processing by both horizontal and vertical-scalar or vector-scalar arrays.

The prediction results are recommended for increasing the interference immunity of detection and decreasing the shift in bearing during generation of the DC in shallow water using towed or stationary (e.g., bottom) horizontal scalar or vector-scalar arrays—when the emitters (noise sources) are located at different depth levels. The individual results of calculations can also be useful for optimizing shallow-water sounding modes of vertical emitting and receiving arrays, which form spatial channels or modes with given numbers in the waveguide.

REFERENCES

1. J. W. Horton, *Fundamentals of Sonar* (US Naval Inst., Annapolis, 1959).
2. M. Ya. Isakovich, General Acoustics (Nauka, Moscow, 1973), [in Russian].
3. G. A. Grachev and G. N. Kuznetsov, Akust. Zh. **31**, 266 (1985).
4. G. N. Kuznetsov and O. V. Lebedev, Acoust. Phys. **58**, 575 (2012).
5. G. N. Kuznetsov and O. V. Lebedev, Gidroakustika, No. 17, 114 (2013).
6. V. A. Shchurov, *Vector Acoustics of Ocean* (Dal'nauka, Vladivostok, 2003) [in Russian].
7. V. A. Gordienko, *Vector-phase Methods in Acoustics* (Fizmatlit, Moscow, 2007) [in Russian].
8. L. M. Brekhovskikh, *Waves in Layered Media* (Nauka, Moscow, 1973) [in Russian].
9. V. A. Zhuravlev, I. K. Kobozev, and Yu. A. Kravtsov, J. Exper. Theor. Phys. **77**, 808 (1993).
10. E. Skudrzyk, *Foundations of Acoustics. Basic Mathematics and Basic Acoustics* (Springer-Verlag, New York, 1971), Vol. 1, Vol. 2.
11. A. N. Stepanov, *Multifield Model of Hydroacoustic Sources* (Samar. Univ., Samara, 2000) [in Russian].
12. G. N. Kuznetsov and A. N. Stepanov, Acoust. Phys. **53**, 328 (2007).
13. D. E. Weston, J. Acoust. Soc. Am. **65**, 647 (1960).
14. C. F. Chien and R. V. Waterhouse, J. Acoust. Soc. Am. **101**, 705 (1997).
15. V. A. Eliseevnin and Yu. I. Tuzhilkin, Acoust. Phys. **47**, 688 (2001).
16. V. M. Kuz'kin, A. V. Ogurtsov, and V. G. Petnikov, Acoust. Phys. **44**, 77 (1998).

Translated by A. Carpenter